Third-harmonic, top-launch, ECRH experiments on TCV Tokamak

S. Alberti 1), G. Arnoux 1), L. Porte 1), J.P. Hogge 1), B. Marletaz 1), P. Marmillod 1), Y. Martin 1), S. Nowak 2), and the TCV Team 1)

1)Centre de Recherches en Physique des Plasmas CRPP EPFL
Association EURATOM-Confédération Suisse
CH-1015 Lausanne, Switzerland
2)Istituto di Fisica del Plasma
EURATOM-ENEA-CNR Association, Milano, Italy

e-mail contact of the first author: stefano.alberti@epfl.ch

Abstract In the moderate magnetic field of TCV (1.5T), the recently installed X3 system (3 gyrotrons @118GHz, 0.45MWeach, 2s) broadens the operational space with the possibility of heating plasmas at high density, well above the cutoff density of the X2 system. To compensate the significantly weaker absorption coefficient compared to the absorption of X2, the top-launch injection allows to maximize the ray path along the resonance layer thus maximizing the optical depth. To maintain the maximum absorption in plasma discharges with a dynamic variation of both density (refraction) and temperature (relativistic shift) a real time control system on the poloidal injection angle has been developped and succesfully tested on TCV. Comparisons of the absorption calculated with the TORAY-GA ray-tracing code and the beam-tracing code, ECWGB, which includes diffraction effects, are presented. An experimental study of the X3 absorption versus plasma density in an L-mode plasma shows that with a total injected power of 1.35 MW full single-pass absorption is reached with a significant fraction of the absorbed power associated to the presence of suprathermal electrons. Compared to ohmic/low-power-heating of ELMy H-modes, it has been possible to enter into a significantly different ELMy regime with an injected power of 1.35MW .

1. Introduction

The recently completed ECH system on the TCV Tokamak, with a total of 4.5MW of installed power (4.1 MW of injected power), and with a highly flexible launching mirror system allowing real time control of the toroidal and poloidal mirror angles, is, at present, the most relevant ECH system for ITER. It consists of 9 gyrotrons grouped in three "clusters" of three gyrotrons each[1]. Two of the clusters operate at 82.7 GHz (0.45MW/gyrotron, 2s) and are used for heating and/or current drive, coupling to the X-mode EC plasma wave from the low-field side and being absorbed at the 2^{nd} harmonic resonance (X2). The third cluster operates at 118GHz (0.45MW/gyrotron, 2s), couples to X-mode from the top of the vacuum vessel and provides the ECH power which is absorbed at the 3^{rd} harmonic resonance (X3)[2].

In the moderate magnetic field of TCV (1.5T), the X3 system broadens the operational space with the possibility of heating plasmas at high density, well above the cutoff density of the X2, where the cutoff for the X2 and X3 waves are 4.2 $10^{19}[m^{-3}]$ and 11.5 $10^{19}[m^{-3}]$, respectively. To compensate the significantly weaker absorption coefficient compared to the absorption of X2, the top-launch injection maximizes the ray path along the resonance layer thus maximizing the optical depth.

2. Experimental setup

As shown in Figure 1, on the left, the three waveguides radiate the rf beams onto a single elliptical mirror. This mirror is made of copper and has a 700mm focal length, focusing the beam inside the plasma. Assuming a gaussian distribution, its minimum waist is w_0 =33mm in E-field. The mirror can be steered radially from 800m to 960mm from pulse to pulse and the

poloidal injection angle θ_l can vary from 40 to 50 degrees during the shot with a maximum speed of 20 deg/s.

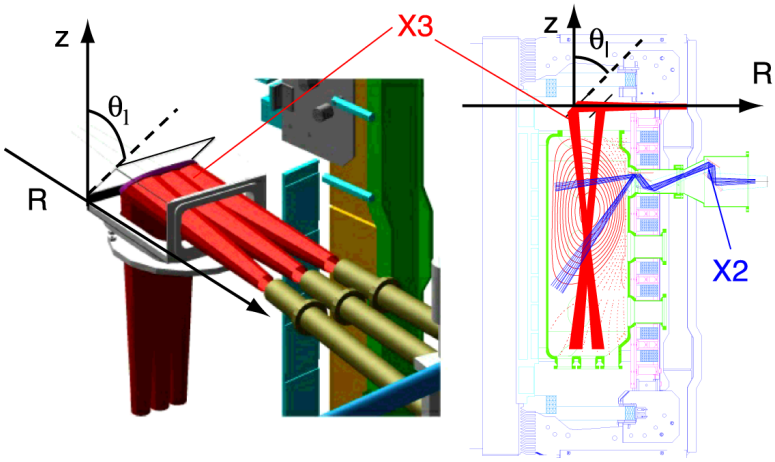

FIG.1. On left side, view of the X3 top-launch mirror. The three RF beams radiated from the HE_{11} waveguides are directed on one single focusing mirror which has radial and poloidal steering capabilities. The poloidal angle, θ_l, can be controlled in real time. On the right side, a poloidal cross section of TCV, with shown, in red, the rf beam paths corresponding to the maximum radial steering range of the X3 launcher. In blue, the poloidal steering range of the X2 launcher.

The main characteristic of the X3 top-launch heating is its sensitivity of the absorption versus poloidal injection angle as it is shown in Figure 2 [2,3,4]. For a given plasma equilibrium shown in Figure 2b) and a fixed launcher radial position, the plasma response versus poloidal injection angle is shown in Figure 2a). With 0.45 MW of injected power, the level of absorption is indicated on this figure by the variation of the central temperature (T_e-X, blue curve) deduced from the soft X-ray emission measurement along a central vertical view line (two-foil method). As a comparison, the calculated absorption with the TORAY-GA code is shown in red. A good agreement between the experiment and the simulation is found.

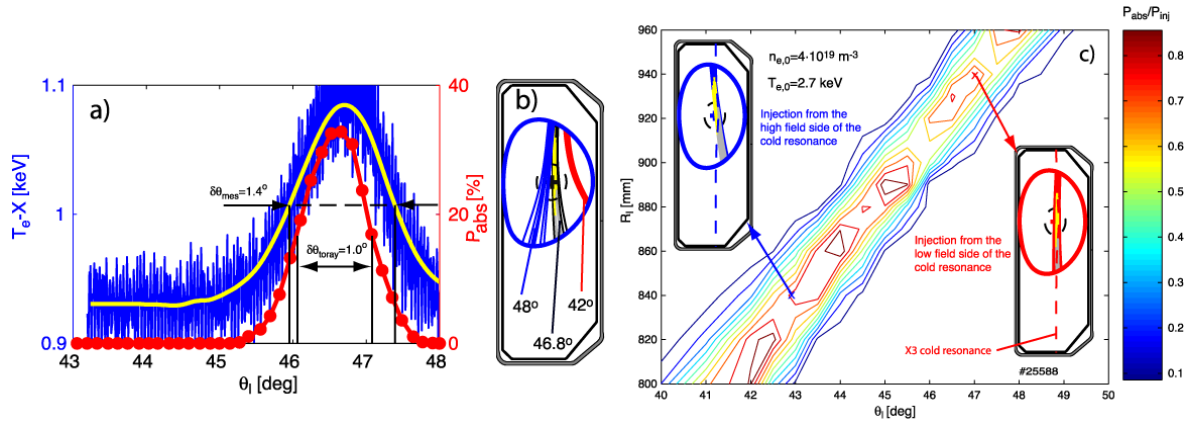

FIG.2. a) Blue trace: plasma temperature, Te-X, versus poloidal injection angle (the yellow trace is the result of low-pass filtering the blue trace). In red, the absorbed fraction as predicted by TORAY-GA. b) Cross section of the plasma with ray trajectories for different injection angles. Contour plot of absorbed fraction versus poloidal injection angle and radial position of the mirror.

The main point to be noticed is the fairly narrow angular range where the X3 wave is absorbed. The calculated X3 top-launch absorption versus poloidal injection angle and radial position of the launcher is shown in Figure 2c). The target plasma cross section is shown in the inserts and the absorption has been calculated on an experimentally obtained plasma equilibrium having a central electron density and temperature of 4 10^{19}m^{-3} and 2.7 keV, respectively. One notices that the FWHM of the absorption versus poloidal injection angle is weakly dependent on the radial position.

3. Real-time feedback on the poloidal injection angle

To maintain the maximum absorption in plasma discharges with a dynamic variation of both density (refraction) and temperature (relativistic shift) a real time control system on the injection angle has been developped. The main element of this feedback system consists in a synchronous demodulation of an harmonic perturbation of the plasma response (line-integrated emissivity of a central soft-X ray chord), generated by sinusoidally varying the launcher injection angle. The dynamic response of the feedback system is related to the maximum frequency at which the mirror can be swept and this frequency has been determined by measuring the transfer function of the system composed by the mirror mechanical system and its motorization. The frequency response of this system is represented in a Bode diagram on Figure 3.

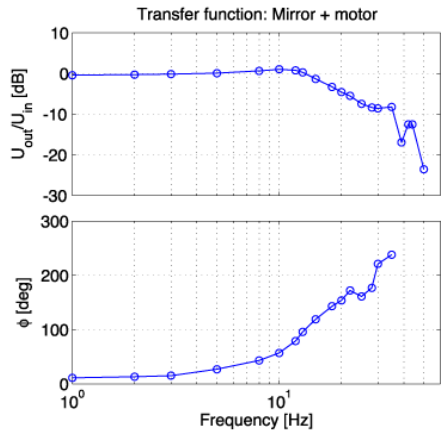

FIG.3. The frequency response of the top-launch mirror system is represented in a Bode diagram. This system consists of the mechanical part and the mirror motorization. The quantities represented in this diagram are the amplitude and phase of the ratio between the desired and actual mirror angular position. A strongly damped resonance is observed around the frequency of 13Hz which is chosen as the driving frequency for the harmonic perturbation.

The schematic of the complete feedback system is shown in Figure 4. In the Laplace transform representation the transfer function shown in Figure 3 corresponds to the function $G_2(s)$. The other elements of this system are detailed in the figure caption. The signal at the output of the low pass filter is proportional to the derivative of the plasma response shown in Figure 2a). The reference, R(s), is set to a value such to maintain the mirror angle on a zero derivative of $dT_e/d\theta$. Only the proportional term of the PID controller has been used in these experiments.

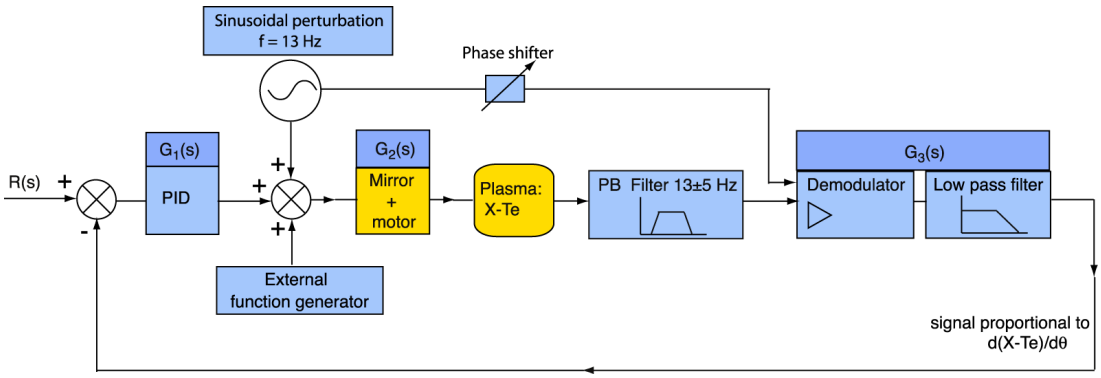

FIG.4. Schematic of the complete closed-loop feedback system. The harmonic perturbation at 13Hz is used both for applying the sinusoidal perturbation on the launcher mirror and also as an input of the synchronous demodulator which is placed after a pass-band filter centered at 13±5Hz. At the output of the demodulator the AC component is filtered out by a low-pass filter (f_{cutoff} = 2 Hz) with the resulting signal being proportional to the derivative of the plasma response function, $dT_e/d\theta$ where θ is the mirror poloidal angle. The dynamic response of the closed-loop system can be adjusted by the parameters of the PID regulator.

The open-loop characteristics of this system are shown in Figure 5, where the time traces of the relevant quantities are represented in a shot on which a linear sweep of the launcher angle is performed. The sweep is such to cross the optimum angle corresponding to the maximum X3 absorption.

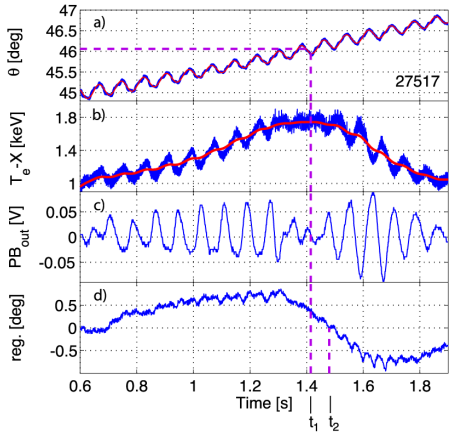

FIG.5. Open-loop signals during a linear sweep of the mirror poloidal angle. Trace a), linear angular sweep of the mirror poloidal angle with superimposed the sinusoidal perturbation at 13Hz. Trace b), Plasma central temperature deduced from the two-foil method using the soft X-ray emission measurement on a central chord. Trace c), Signal at the output of the pass-band filter whose envelope is proportional to the derivative $dT_e/d\theta$ of the Te-X signal. Trace d), signal at the output of the low-pass filter following the demodulator. The error signal, which is fed to the PID controller, is obtained by substracting this signal from the reference signal.

One notices that the envelope of the signal at the pass-band filter output (Trace c) crosses zero exactly at the time (t_1=1.41s) where the mirror is at the optimum angle. The small time delay between this time and the time of zero crossing of trace d) (t_2=1.47s) is caused by the low-pass filter. This small difference can be compensated by properly adjusting the level of the reference signal R(s).

The closed loop characteristics of the real-time feedback are shown in Figure 6. In this shot the mirror poloidal angle was pre-programmed to perform a linear sweep across the angular region of optimum heating (green line). The feedback controlled mirror-angle (red line) has been such to reach the optimum angle faster than the pre-programmed sweep and, once the optimum angle has been reached (t = 1.1s), the feedback has reacted such to maintain this optimum angle despite the externally imposed ramp, forcing the mirror to move away from the optimum. In the experiments with feedback performed so far only the proportional term of the PID controller was used. After an experimental optimisation of the different parameters in the system, a stable real-time control of the optimum injection angle of the X3 launcher has been obtained on a wide variety of L-mode plasmas.

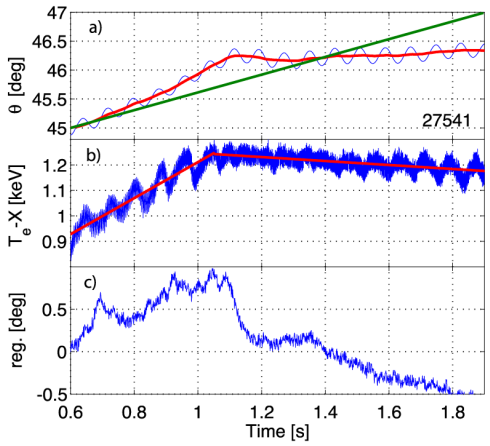

FIG.6. Real-time control of the mirror in a L-mode plasma. In this shot the mirror angle was programmed with a linear sweep (green line) across the optimum injection angle which occurs at t =1.1s. The error signal which is fed to the proportional controller is shown on trace c. On trace b), the time-trace of the central plasma temperature clearly demonstrates that once the launcher optimum angle is reached, the feedback controls the launcher such to maintain it on the optimum angle.

Further development of this real time control system are required in case of plasmas with an L-H transition and H-mode plasmas where the perturbations associated to the presence of ELMs and also rapid density variations strongly perturbe the feedback loop. A complete modeling of the system will allow to further optimize the dynamic response of the real-time

control. Once the Advanced Plasma Control System of TCV will be operational it is also planned to transform this analog controller to a digital one.

4. X3 Absorption with top-launch

The X3 absorption studies were significantly simplified with the real-time control of the launcher and the absorbed fraction versus plasma density at different levels of the injected rf power has been measured. With the mirror feedback control, the absorbed rf power was measured only after a stationary state of the mirror angle was reached. The absorbed fraction was measured during a modulated portion of the X3 rf pulse (full-power modulation of one gyrotron at 237Hz) using a diamagnetic loop [5].
The absorbed fraction versus plasma density is shown in Figure 7b, for two different levels of average injected rf power and a L-mode target plasma with a cross section as shown in the insert of Figure 2c (R_0 = 0.88m, a = 0.26m, κ = 1.6, δ =0.1, B_T = 1.45T, I_p = 230kA). The two levels of average injected power correspond to the sum of the average power of a fully square-wave modulated gyrotron (P_{av} = 225kW) plus the power of one (450kW) or two (900kW) additional gyrotrons.
The difference between the measured absorbed fraction (DML) and the one predicted by the TORAY-GA code is to be associated with the existence of a suprathermal population generated by the X3 wave itself and not taken into account in TORAY-GA. At higher electron densities this difference is lower since a fast thermalization of the suprathermal population occurs. The coupling to the ions (equipartition) is very weak since the average ion temperature, on a vertical chord, remains nearly constant at T_i = 510eV during the entire plasma shot.

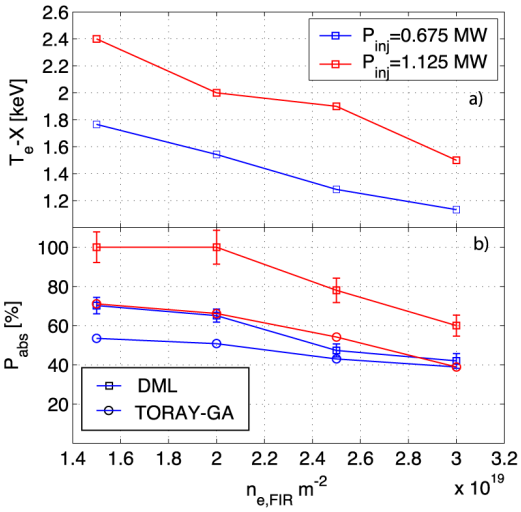

FIG.7. a) Central temperature versus line integrated density for two levels of X3 injected power. For the target plasma used, the value of the central density [m^{-3}], is twice the value of the line integrated density. The central temperature during the ohmic heating (before rf injection) is 0.9 keV.
b) Absorbed fraction measured with the DML (squares) and predicted by TORAY-GA (circles) versus line integrated density for two levels of X3 injected power (0.675MW and 1.125MW).

The typical density and temperature profile measured with the Thomson scattering diagnostic are shown in Figure 8 for a central electron density of 4.10^{19} m^{-3} which, on Figure 7, corresponds to a line integrated density of 2.10^{19} m^{-2}. The ohmic profiles (squares) are time averaged during 100ms before the X3 is turned on and the profiles during the ECH phase are time averaged from the start of the ECH pulse until the modulation phase is started. At the X3 power switch on, a clear flattening of the density profile is observed. This "pumpout" phenomenon has also been observed on X2 ECH and ECCD experiments on TCV [6] as well as on ASDEX Upgrade [7].
For the plasma target used in this study, a contour plot of the absorbed power fraction, calculated with TORAY-GA, versus central density and temperature is shown in Figure 9. The presence of a suprathermal electron population is not taken into account in this

calculation.The four inserts show the ray trajectories inside the plasma for the extremities of the density and temperature ranges.

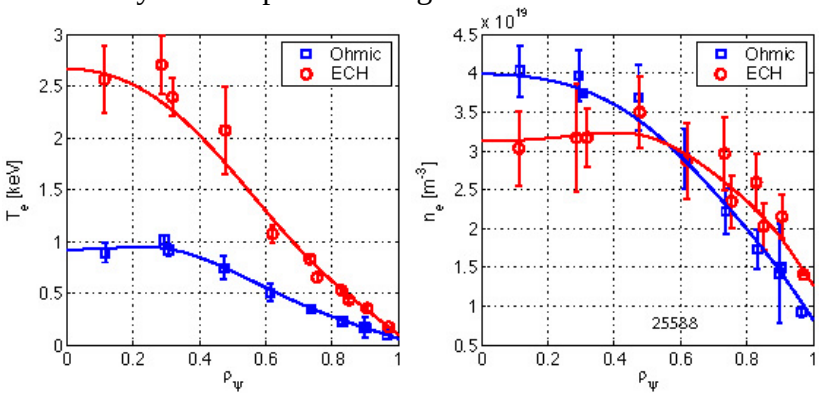

FIG.8. The temperature and density profiles measured with the Thomson scattering diagnostic for both ohmic and ECH phases. This shot corresponds to a point in Figure 7 with P_{inj} =1.125MW and line integrated density of 2.10^{19} m^{-2}.

The yellow part on each ray indicates the absorbed fraction between 10% and 90% of the total absorbed fraction for each specific ray. The cold resonance is indicated by the vertical dashed line and the q=1 surface by the circular dashed line.

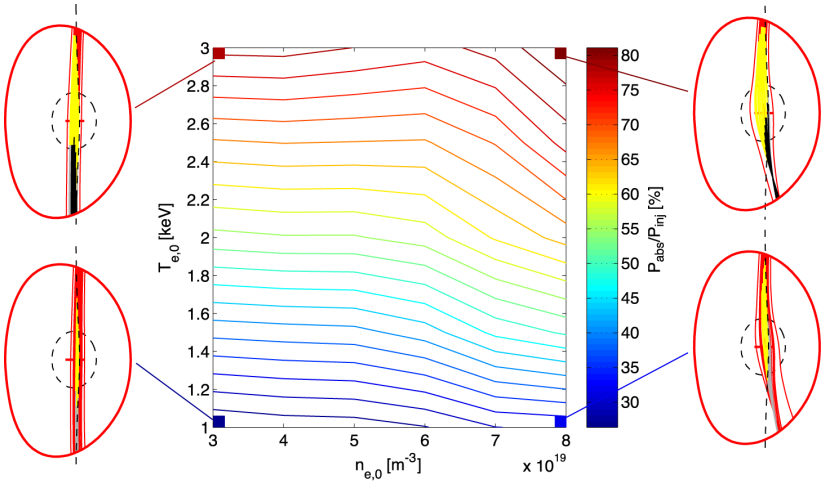

FIG.9. Contour plot of the absorbed power fraction calculated with TORAY-GA versus central plasma density and temperature. The equilibrium corresponds to shot 25588 and the calculation with TORAY-GA have been made by properly scaling the respective density and temperature profiles.

As expected, a strong dependence of the absorption on the electron temperature is observed, whereas the dependence on density is fairly weak. At high density, refraction effects can generate a fairly strong focusing of the rf beam. In this cases the WKB approximation, on which the ray-tracing code is based, might fail. In order to assess the importance of diffraction effects on the X3 power absorption, preliminary studies with the beam tracing code ECWGB [8] have been performed. In Figure 10 a comparison between the two codes is made. The launcher mirror has been designed [2] to be focusing inside the plasma with a minimimum waist located approximately at the vacuum vessel center.

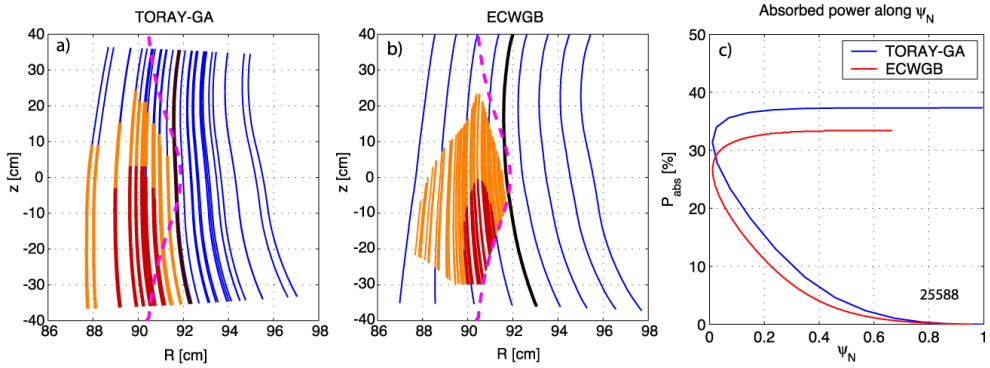

FIG.10. Comparison of the ray trajectories for the TORAY-GA (a) and ECWGB (b). On (c), the total absorption computed along the central ray (indicated in black on a) and b)) is shown in red for the ECWGB code and in blue for the TORAY-GA code.

In TORAY-GA, the focusing gaussian beam is approximated by a cylindrical beam with a gaussian rf power distribution of width $w_0/\sqrt{2}$. The ray trajectories of Figure 9 a,b show this effects especially for the case of ECWGB where the rf beam in the absorption region (described by the red colored rays) is slightly diverging which is consistent with a focusing beam having its minimum waist located at z ≈ 20cm. The slightly higher absorption predicted by TORAY-GA might be explained by the cylindrically shaped modeling of the rf beam.

Further comparisons between the two codes are presently underway especially for the cases where, at high density, refraction effects cause additional focusing (as shown in Figure 8).

5. X3 top-launch heating of quasi-stationary ELMy H-mode plasma

Until X3 heating was installed on TCV the only quasi-stationary H-modes that were routinely available were ohmic H-modes that were approached through a narrow gateway in parameter space [9]. Using X3 to heat the core of ELMy H-modes, accessed through the gateway, experiments have been performed to establish quasi-stationary additionally heated ELMy H-modes and to study the effect of heating on the ELMs. Initial results of X3 heating in quasi-stationary ELMy H-mode plasmas were presented by Porte et al. [10]. In this reference, results of low power X3 ECH ($P_{ECH,X3} < P_{\Omega,}$ where $P_{ECH,X3}$ is the X3 absorbed power and P_Ω is the ohmic power) have shown that the ELM frequency was reduced with increasing $P_{ECH,X3}$ but they were unable to alter the ELMy regime (i.e. the ELM type).

In recent experiments, $P_{ECH,X3} \approx 3P_\Omega$ has been obtained and the results are significantly altered as compared to [10]. It has been possible to enter into an ELMy regime that is fundamentally different to ohmic/low-power-heating ELMy H-modes. The ELM frequency is reduced and the energy loss per ELM is significantly increased (≈ factor of 10). There seems to be a minimum additional heating power before the transition from one ELM regime to another can be achieved as it is demonstrated in Fig.11 when, at t=1.42s, one gyrotron is switched off.

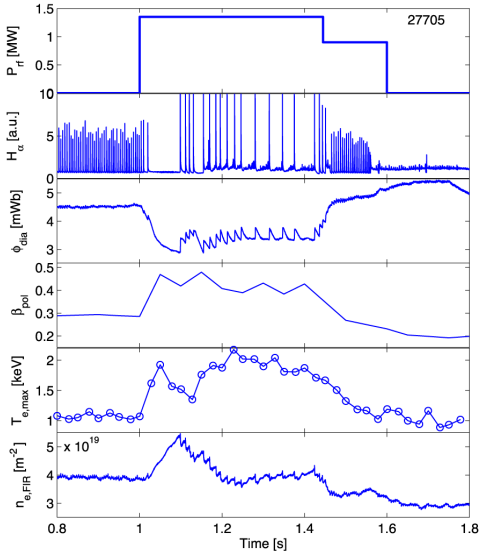

FIG.11: Temporal evolution of a quasi-stationary ELMy H-mode plasma, heated using top launch X3. The discharge exhibits a clear transition from one ELMy regime to another with the addition of X3 heating. The two ELMy regimes are distinguished by their ELM frequency and amplitude and by their effect on the stored energy. ELMs in the additionally heated phase cause an energy loss per ELM that is ≈10 times more than in the ohmic phase. At t≈1.42s one of the X3 gyrotrons was switched off and the plasma immediately went back to the ohmic/low power ELMy regime..

In Figure 11 a discharge is presented where the transition from the 'low-power' regime to the 'high-power' regime is achieved. With a total injected power of 1.35MW, the absorbed rf power during the quasi-stationary part of the discharge with large ELM's (t =[1.2-1.42s]), is in excess of 850kW. Work continues to determine the ELM type, according to the usual classification and to establish a technique to make the high-power ELMy regime easily and routinely accessible.

Further studies of the X3 absorption properties both in L and H-mode plasmas at higher elongations and triangularities will be investigated in the near future.

6. Conclusions

A top-launch X3 ECH system has been installed on TCV in order to heat high density plasmas. The X3 absorption is theoretically predicted to be strongly sensitive to the launcher poloidal angle. This strong dependence has been experimentally confirmed showing a typical launching angular width of $\pm 0.5^0$ (FWHM) within which the absorbed power fraction is maximized. This narrow width together with the goal of maintaining the optimum absorption in dynamically varying plasma conditions has motivated the development of a real–time control system of the launching angle. This system has been successfully tested and has allowed to perform extensive absorption studies in L-mode plasmas. With a total injected power of 1.35MW, full-single pass-absorption has been reached with a significant fraction of the power absorbed on a suprathermal population. Preliminary comparisons between the linear ray-tracing code TORAY-GA and the beam-tracing code ECWGB have been presented. First experiments with 1.35MW of injected power have demonstrated the accessibility to an ELMy regime that is fundamentally different to ohmic/low-power-heating ELMy H-modes.

Acknowledgement: This work was partially supported by the Swiss National Science Foundation

Appendix 1: References

[1] T. Goodmann et al., "Design and installation of the electron cyclotron wave system for the TCV tokamak",Fusion Technology (Proc. of 9th Symp. Lisbon 1996), North-Holland, Amsterdam (1997), 565.

[2] J.P. Hogge et al., "Preliminary results of top launch third harmonic X-mode electron cyclotron heating in the TCV tokamak",Nucl. Fusion, **43** (2003)1353.

[3] G. Arnoux et al., "Top-Launch X3 ECH and its use as an electron energy diagonstic on the TCV Tokamak", IAEA Technical Meeting on ECRH, Klosterseeon, July 2003.

[4] G. Arnoux et al., "Third-harmonic X3 absorption in a top launch configuration on the TCV tokamak, Submitted for publication

[5] A. Manini et al., "Modulated ECH power absorption measurements using a diamagnetic loop in the TCV tokamak", Plasma Phys. Control. Fusion, **44** (2002) 139.

[6] A. Zabolotsky et al.,"Observation and empirical modelling of the anomalous particle pinch in TCV",Plasma Phys. Control. Fusion, **45** (2003) 735.

[7] C. Angioni et al., Density response to centrel electronheating: theoretical investigations and experimental observations in ASDEX Upgrade, Nucl. Fusion, **44** (2004)827.

[8] D. Farina et al., "ECWGB: a beam tracing code for EC heating and current drice",IFP-CNR Internal Report FP 03/6, October 2003.

[9] Y. Martin et al.,"ELMing H-mode Accessibility in Shaped TCV Plasmas"; Proceedings of the 18th IAEA Conference on Fusion Energy, Sorrento, Italy, October 14–19 ; 2000.

[10] L. Porte et al.,"Third Harmonic X-mode Electron Cyclotron Resonance Heating on TCV using Top Launch ", Proceedings of the 19th IAEA Conference on Fusion Energy; Lyon, France, paper # EXP5-15